ORIGINAL PAPER

Efficacy of impregnated active carbon in manganese removal from aqueous solutions

Didar Zohreh[1,✉], Fatemeh Abedi[2]

1. Assistant professor of food science, Department of food science, Neyshabur branch, Islamic Azad University, Neyshabur, Iran
2. PhD of analytical chemistry, Islamic Azad University, Neyshabur, Iran

Date of submission: 25 Apr 2018, ***Date of acceptance:*** 26 Feb 2019

ABSTRACT

Adsorption is a chemical method for water purification. In the present study, native and impregnated active carbon was used for adsorption to evaluate the efficacy of the process in manganese removal from aqueous solutions. Impregnation reaction was performed using the precipitate colloids of manganese oxides onto the carbon surface. X-ray diffraction, Fourier-transform infrared spectroscopy, and scanning electron microscopy confirmed that the process was appropriate for carbon impregnation. The experiments indicated that the highest adsorption of Mn^{2+} ions by impregnated active carbon occurred at the pH of 9 (Mn^{2+} removal: 67.19%). In addition, the reaction time, mixing rate, and adsorbent dosage affected the efficacy of adsorption, and optimal results were obtained at the reaction time of 100 minutes, mixing rate of 100 rpm, and adsorbent dosage of 4 mg/l. In all the test conditions, impregnated active carbon had better performance in Mn^{2+} removal from aqueous solutions compared to native active carbon (99% confidence level). The Langmuir and Freundlich isotherm models were also applied to evaluate the adsorption process. Accordingly, R_L was 0.07 and 0.027 for raw active carbon and impregnated active carbon, respectively. R_L magnitude confirmed the suitability of the Langmuir model for Mn^{2+} adsorption using impregnated active carbon. According to the results, impregnated active carbon exhibited the maximum adsorption capacity (q_{max}) of 20.53 mg/g, while this value was estimated at 6.62 mg/g in raw active carbon. On the other hand, the adsorption kinetic analysis indicated that the pseudo-second order mode and intra-particle diffusion model could be used for this process.

Keywords: Manganese, Carbon, Adsorption, Kinetics, Water

Introduction

Manganese in water sources is considered to be a pollutant due to its adverse effects on the color of water and causing turbidity. With conversion into insoluble forms (Mn[III] and Mn[IV]),[1] precipitation on pipeline causes a black-brown appearance in water. Therefore, the removal of manganese from water is of utmost importance.[2] The main issue associated with the presence of manganese in water sources is manganese deposition on filter media,[3] concrete tanks,[4] and distribution systems. Chemical and microbial oxidation could lead to the deposition of manganese, which occurs at the high concentrations of this element.[5]

Several processes have been proposed for the removal of manganese, such as physical, chemical, and biological processes. Active carbon is a material that has been extensively investigated for the elimination of water pollutants.[6-8]

Use of solid surfaces is an alternative approach for the sorption of Mn(II). Metal oxide surfaces are typically applied as solid surface, especially manganese oxide.[9, 10] According to the standards of the Environmental Protection Agency (EPA) standards, the concentration of Mn^{2+} should not exceed 0.05 mg/l.[11] Oxidizing components (e.g., $KMnO_4$, Cl_2, and ozone) could be used for the removal of manganese.[12]

To the best of our knowledge, no prior research has investigated the effect of impregnated active carbon with MnO_2 on the

✉ *Didar Zohreh*
z_didar57@yahoo.com

Citation: Didar Z, Abedi F. Efficacy of impregnated active carbon in manganese removal from aqueous solutions. J Adv Environ Health Res 2019; 7(2): 113-121

removal of Mn^{2+} from aqueous solutions. The present study aimed to eliminate manganese ions from water through the adsorption process under various circumstances.

Materials and Methods

In this study, all the reagents were of the analytical grade and purchased from Merck Company, Germany.

Preparation of impregnated carbon

Impregnated carbon was prepared through a reductive reaction,[11] during which the colloids of manganese oxide were precipitated on the carbon surface based on Equation (1), as follows:

$$2KMnO_4+8HCl = 2MnO_2+2KCl+3Cl_2+4H_2O \quad (1)$$

Active carbon was placed on $KMNO_4$ solution. Drop wise addition of hydrochloric acid (37.5% W_{HCl}/W_{H2O}) was also carried out at this stage. After stirring using a magnetic stirrer (model: VELP) for one hour, the suspension was filtered, washed several times with distilled water in order to remove free potassium and chloride ions, and dried.

The concentrations of manganese ions were measured using an atomic absorption spectrophotometer (Varian AA240), and the results were expressed as mg/l. The pH of the solution was determined using the ATC pH meter (model: GP353).

Characterization of active carbon

Energy Dispersive X-ray Spectroscopy (EDS

Energy dispersive X-ray spectroscopy (EDS) was performed based on the interaction of the electron analysis source with the samples so as to verify the presence of the elements in the samples.[13]

X-ray powder diffraction (XRD)

X-ray powder diffraction (XRD) was conducted using a Phillips PW1820 diffractometer within the temperature range of 2-80 ºC.

Morphological features of active carbon

To investigate the morphological features of both forms of active carbon (native and impregnated), images were obtained via scanning electron microscopy (SEM; model: Phenom ProX) with the magnification of 6,000. The scanning speed of the samples in the electron microscope was 8° in minutes, with the refractive angle range of 10-70.

Fourier-transform infrared spectroscopy (FTIR)

The Fourier-transform infrared spectroscopy (FTIR) spectra of native and impregnated active carbon were analyzed before and after the adsorption process using the Perkin-Elmer FTIR spectrophotometer (model: Spectrum Two) within the range of 500-4,000 1/cm using KBr disks.

Adsorption experiments

The experiments were conducted in glass flasks (volume: 0.1 l) at the temperature of 25 ºC and mixing rate of 100 rpm. The selected circumstances for the kinetic experiments were the blending of the active carbon (concentration: 4 g/L) with 100 milliliters of a solution containing 120 mg/l of Mn^{2+}, which was mixed at 100 rpm several times (50-300 minutes) at the initial pH of 9. Afterwards, the supernatant was filtered.

To assess the absorption of manganese on active carbon, the same steps were taken with the experiment time of 300 minutes (sufficient for achieving chemical equilibrium). In addition, the impact of pH on Mn^{2+} removal was evaluated at various pH levels (range: 3-10). All the experiments were performed in duplicate.

Equilibrium modeling of Mn^{2+} adsorption

The Langmuir adsorption model was used in the form of the following equation:[14]

$$\frac{1}{q_e}=\frac{1}{q_{max}b}\times\frac{1}{C_e}+\frac{1}{q_{max}} \quad (2)$$

where: q_e is the equilibrium adsorption capacity (mg/g), C_e represents the equilibrium concentration (mg/l), q_{max} shows the maximum concentration of the adsorbed Mn^{2+} per unit weight of the adsorbent (mg/g), and b is the Langmuir constant (l/mg).

The Langmuir parameters (q_{max} and b) were measured based on the slop and intercept of the

linear plots of $1/q_e$ versus $1/C_e$

$$R_L=\frac{1}{1+K.Co} \quad (3)$$

The Freundlich adsorption model was considered based on Formula 4, as follows: [14]

$$\log(q_e)=\log K_f+\frac{1}{n}\log(C_e) \quad (4)$$

where: K_f is the adsorption capacity, and *1/n* represents the adsorption intensity as the Freundlich constants. In addition, the magnitude of K_f and *1/n* was determined based on the slop and intercept of the linear Freundlich plot of log (q_e) versus log (C_e).

Adsorption kinetics

The general equation for the pseudo-first-order was as follows: [14]

$$\log(q_e-q_t)=\log q_e-\frac{K_{ads}}{2.303}t \quad (5)$$

where q_e is the amount of the adsorbed Mn^{2+} per unit mass of the adsorbent in the equilibrium state (mg/g), q_t denotes the amount of the adsorbed Mn^{2+} per unit mass of the adsorbent at time (mg/g), and k_{ads} shows the adsorption rate constant for Mn^{2+} adsorption, which was measured based on the slop of the linear plot log (q_e-q_t) versus time (t).

The pseudo-second-order model was considered based on Formula 6, as follows: [14]

$$\frac{t}{q_t}=\frac{1}{h}+\frac{t}{q_e} \quad (6)$$

where *h* is the initial sorption rate (mg/g min). The values of q_e(1/slope) and h(1/intercept) could be determined based on the plot of t/q_t versus *t*.

The intra-particle pore diffusion model was measured based on Equation 7, as follows:

$$q_t=K_i\,t^{\frac{1}{2}} \quad (7)$$

where *ki* denoted the intra-particle pore diffusion rate constant (mg/g min), and q_t is the magnitude of the adsorbed Mn^{2+} per unit mass of the adsorbent at *t*, which was plotted as a function of the square root of *t*.[1, 2]

Statistical analysis

All the tests were conducted in duplicate, and the mean values were calculated. Data analysis was performed using ANOVA in the STATISTICA software at the significance level of $P\leq0.01$.

Results and Discussion

Physical properties of active carbon

Figure 1 shows the FTIR spectra of various active carbon.

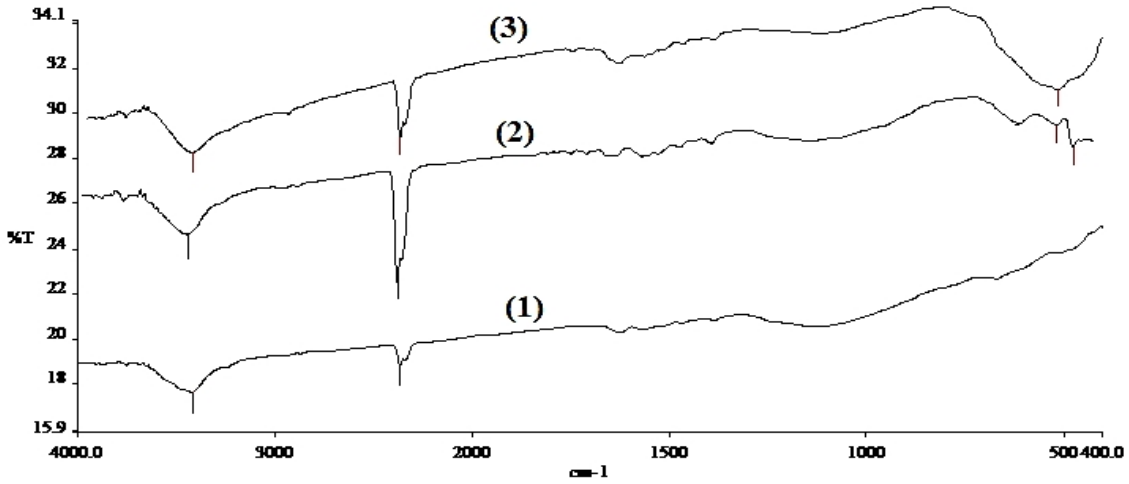

Fig. 1. FTIR spectra of 1) raw active carbon, 2) impregnated active carbon, and 3) impregnated active carbon after adsorption

All the analyzed spectra depicted a marked transmittance band at approximately 3,418 1/cm, which could be attributed to the O-H stretching mode of hydroxyl groups.[15] The bands close to 2,366 1/cm ascended to the carbon-oxygen groups due to ketone.[16] The

impregnated active carbon exhibited two bands at 515 and 480 1/cm, the presence of which was obviously associated with the Mn-O bond, confirming that the impregnation of active carbon by manganese oxide had occurred.[17] After adsorption, the impregnated active carbon exhibited an extra band at 515 1/cm, which corresponded to the Mn-O bond.[17]

Before and after adsorption, the micrographs of raw active carbon and impregnated active carbon were obtained at the magnification of 10,000X. Furthermore, the observations confirmed the deposition of manganese oxide on active carbon. As can be seen in Figure 2-c, after the adsorption process, the magnitude of the deposited manganese oxide increased as was evident in the EDS observation (Figure 2). These observations implied the impregnation of manganese on the surface of active carbon.

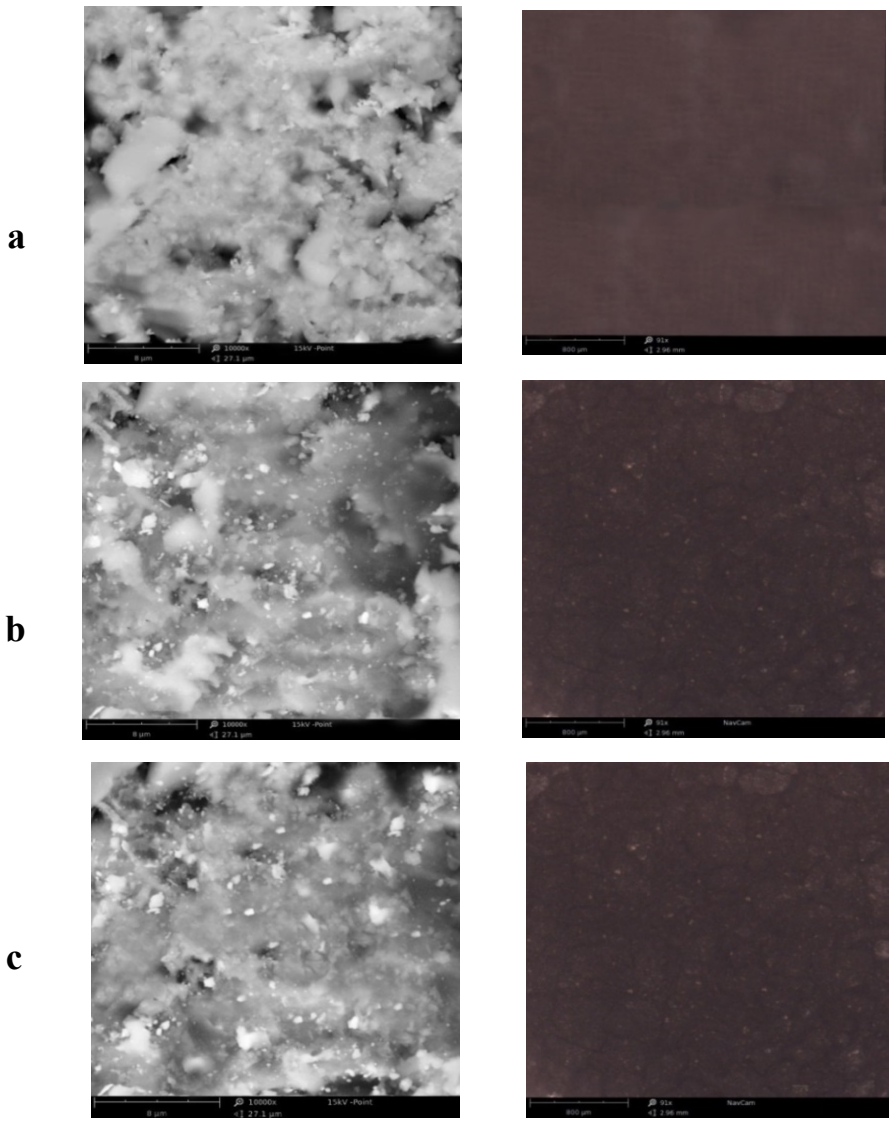

Fig. 2. SEM and EDS of a) raw active carbon, b) impregnated active carbon, and c) impregnated active carbon after adsorption

The EDS peaks of the native and impregnated active carbon are depicted in Figure 4. Accordingly, the impregnation of manganese on active carbon occurred. In addition, the observations indicated that after the absorption process, the amount of manganese oxide increased on the impregnated active carbon (Figure 3).

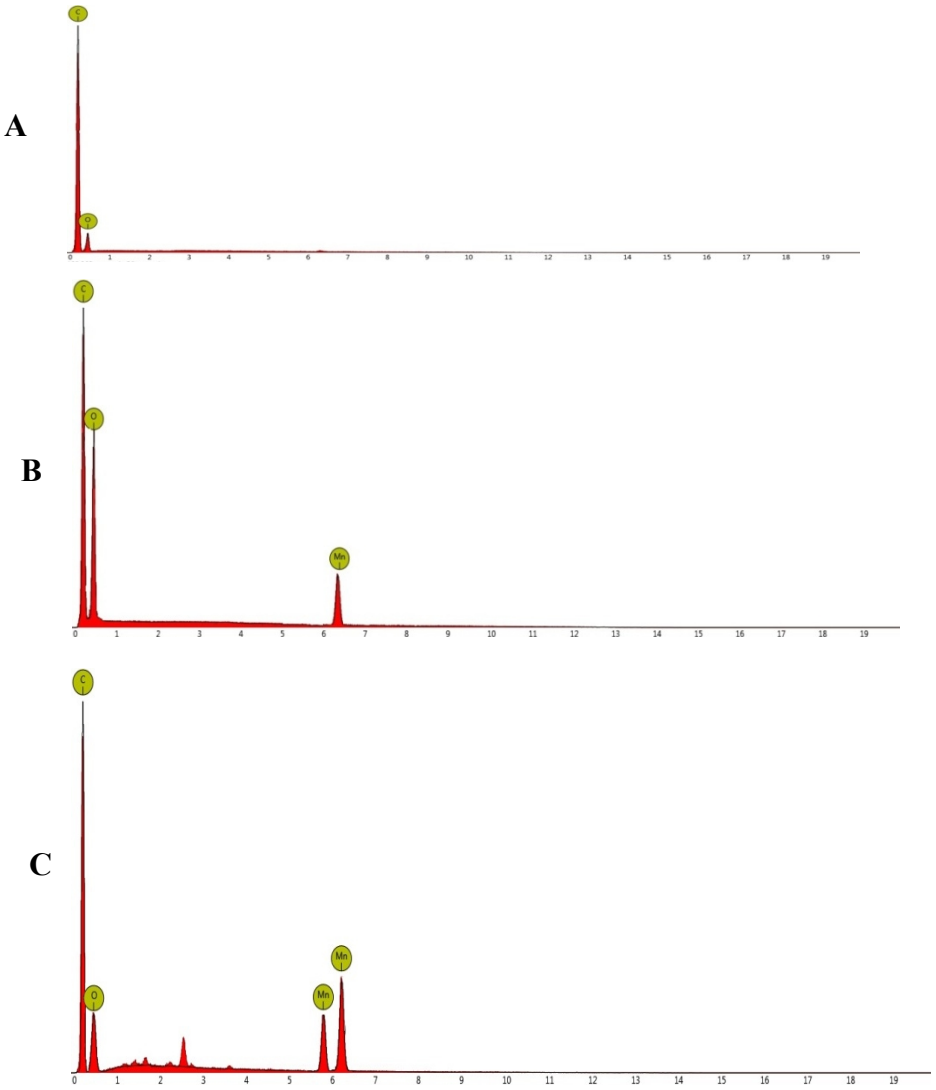

Fig. 3. EDS of a) raw active carbon, b) impregnated active carbon, and c) impregnated active carbon after adsorption

The patterns of native and impregnated active carbon implied the formation of manganese oxide. The impregnated active carbon presented the peaks at 2Θ of 23º and 36º (Figure 4). According to the ICDD 00-012-0720 data, the peaks appeared at 2Θ of 23º and 36º, indicating the presence of manganese oxide.[18]

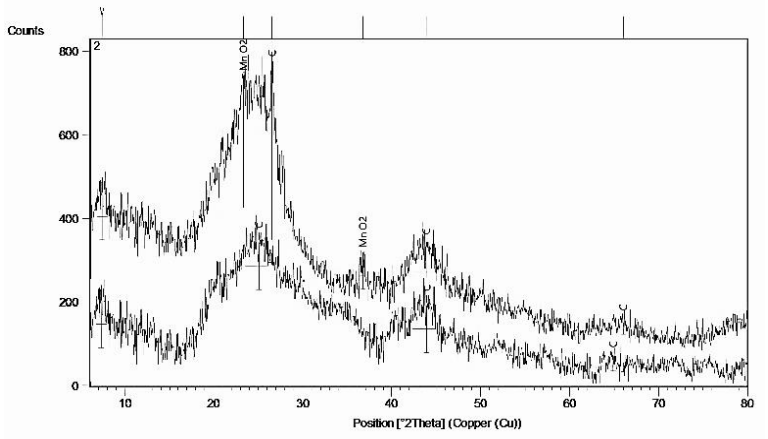

Fig. 4. X-ray diffraction (XRD) patterns of raw and impregnated active carbon

Adsorption experiments

The results of the adsorption experiments are summarized in Table 1. Accordingly, all the tested parameters had significant effects on the removal efficacy of manganese using the impregnated active carbon.

Effect of pH on the adsorption of Mn^{2+} by the impregnated active carbon

Figure 5 shows the rate of manganese removal at various pH levels. Accordingly, the highest Mn^{2+} ion adsorption by the impregnated active carbon occurred at the pH of 8-9. In addition, increased pH resulted in the improved efficacy of Mn^{2+} removal, which could be attributed to the competition between H^+ and Mn^{2+} at lower pH levels, which inhibited ion exchange on the surface of the impregnated active carbon.

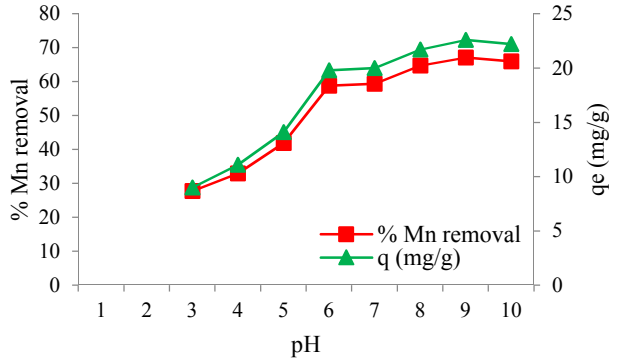

Fig. 5. Effect of pH on Mn^{2+} removal by impregnated active carbon (C_0=120 ppm, T=25 ºC, mixing rate=100 rpm, active carbon=4 g/l)

The most probable mechanism for Mn^{2+} adsorption by the impregnated active carbon was considered to be the ion exchange between H^+ and Mn^{2+}.[19]

According to the findings, increased pH improved the removal efficacy of Mn^{2+} from water, which could be due to the competition between H^+ and Mn^{2+} in acidity.[11] In this regard, Da Silveria reported the optimal pH for Mn^{2+} removal to be 9.[24] On the other hand, decreased acid concentration enhanced the deposition of MnO_2 on active carbon, while higher acid concentrations inhibited the formation of MnO_2.

Adsorption of manganese at various process times, initial active carbon dosages, and mixing rates

Table 1 shows the effects of various factors on the efficacy of Mn^{2+} adsorption by the impregnated active carbon**.**

Table 1. Effect of experimental parameters on Mn^{2+} removal by impregnated active carbon

Experimental parameters		% Mn removal
Time (min)	50	65.49667^{c}
	100	67.22667^{a}
	150	66.48667^{b}
	200	66.51^{b}
	250	66.54^{b}
	300	66.52^{b}
Mixing rate (rpm)	100	67.75333^{a}
	200	57.64333^{b}
	300	42.33333^{c}
Adsorbent dosage	1	33.39333^{e}
	2	40.40667^{d}
	3	50.57^{c}
	4	67.19333^{a}
	5	66.26667^{b}
	6	66.29333^{b}
pH	3	26.22333^{h}
	4	32.58333^{g}
	5	41.58667^{f}
	6	58.61333^{e}
	7	59.22^{d}
	8	64.76^{c}
	9	67.19333^{a}
	10	65.50667^{b}

Increasing the process time to 300 minutes was associated with the higher magnitude of the adsorbed manganese, while the process time of more than 300 minutes was associated with no extra efficacy in manganese removal. This might be due to the occupation of active sites at extended process times.

The adsorption capacity (mg/g) of Mn^{2+} at various dosage of active carbon is presented in Table 1. Accordingly, the amount of adsorbed Mn^{2+} increased from 33.39% to 67.19% at the adsorbent dosages of 1-4 g/l, respectively. Evidently, increasing the adsorbent dosage incremented the available active sites for Mn^{2+} adsorption.

In a research in this regard, Taffarel reported that at higher concentrations of impregnated zeolite, the removal rate of Mn^{2+} was higher.[11] However, the adsorbent dosages

of higher than 4 g/l had no extra efficacy in Mn^{2+} removal due to the low concentration of remaining manganese in the solution to be adsorbed. On the other hand, Izlen Cific *et al*. investigated the efficacy of Fe-impregnated pumice composite in the removal of manganese, reporting that the impregnation process led to the higher efficiency of pumice composite in the removal of manganese.[25]

Mixing rate was another influential factor in the removal of Mn^{2+} (Table 1). According to the obtained results, increased mixing rate led to the lower efficacy of Mn^{2+} removal. The most possible interpretation was that the high mixing rate could interfere with the adsorption process. Accordingly, 100 rpm was considered to be the optimal mixing rate for the removal of Mn^{2+} (Table 1).

Adsorption isotherms

The equilibrium experiments were conducted at the pH of 9, initial adsorbent dosage of 120 ppm, process time of 100 minutes, and mixing rate of 100 rpm. The Langmuir and Freundlich isotherm models were selected to investigate the adsorption process. Furthermore, the adsorption kinetics were assessed based on the pseudo-first-order, pseudo-second-order, and intra-particle pore diffusion model (Table 2).

Table 2. Adsorption isotherm parameters in Mn^{2+} adsorption onto active carbon

	Langimuir model				Freundlich model		
	q_{max} (mg/g)	b	R^2	R_L	K_f	1/n	R^2
Natural active carbon	6.62	0.1	0.89	0.07	1.085	1.33	0.94
Impregnated active carbon	20.53	0.3	0.86	0.027	6.085	0.25	0.96

According to the information in Table 2, the impregnated carbon exhibited better performance compared to native carbon. In addition, q_{max} in the Langmuir model (maximum adsorption capacity of carbon) and K_f in the Freundlich model (adsorption energy) were significantly higher with the impregnated active carbon compared to native carbon. Therefore, impregnation positively influenced manganese removal. In the present study, the adsorption capacity of the impregnated active carbon was 20.53 mg/g, which is consistent with the findings of Gallios, indicating that the adsorption capacity of the impregnated active carbon was 19.35 mg/g.[8]

In the current research, R_L was estimated at 0.07 and 0.027 for native and impregnated active carbon, respectively. Based on the R_L magnitude, the suitability of the Langmuir model for Mn^{2+} adsorption by impregnated active carbon was confirmed, while the higher R^2 in the Freundlich model indicated that this model is more appropriate for Mn^{2+} sorption by native active carbon. Moreover, the results obtained based on the Freundlich model demonstrated the multilayer adsorption of manganese by the impregnated active carbon.[26]

Adsorption kinetics

In the present study, three adsorption models (pseudo-first-order, pseudo-second-order, and intra-particle pore diffusion model) were applied to interpret the experimental data and obtained results (Table 3).

Table 3. Kinetic constants of Mn^{2+} adsorption onto active carbon

	Pseudo- First order model				Pseudo- second order model			Intra- particle diffusion model	
	$q_{e\ (exp)}$ (mg/g)	K_{ads}	$q_{e\ (theor)}$ (mg/g)	R^2	h	$q_{e\ (theor)}$ (mg/g)	R^2	K_i	R^2
Natural active carbon	6.45	0.011	4.22	0.82	0.32	6.54	0.992	0.5	0.88
Impregnated active carbon	21.3	0.035	7.9	0.86	0.76	22.27	0.997	2.51	0.98

According to the information in Table 3, the adsorption of Mn^{2+} by the impregnated active carbon did not correspond to the pseudo-first reaction. Additionally, the comparison of the calculated q_e values with the experimental values of q_e indicated that the pseudo-first-order

kinetic model was not suitable for this experiment.

In the current research, significant difference were observed between the experimental and theoretical values of q_e and the low R^2 in the pseudo-first-order model, which confirmed that this model is not suitable to assess the kinetics of manganese adsorption on active carbon. In contrast, the pseudo-second-order and intra-particle diffusion models were considered appropriate in this regard (Table 3).

Conclusion

According to the results, the adsorbed Mn^{2+} increased at high pH (9-10), with the adsorption kinetics fitting the pseudo-second-order and intra-particle diffusion models. Furthermore, both the Freundlich and Langmuir models properly matched the equilibrium data, implying the presence of monolayer adsorption and heterogeneous surface existence in the impregnated active carbon (maximum capacity: 20.53 mg/g).

Acknowledgements

Hereby, we extend our gratitude to the Food laboratory Center of Islamic Azad University, Neyshabur Branch, Iran and all the colleagues for assisting us in this research project.

References

1. Zapffe C. The history of manganese in water and methods for its removal. J Am Water Works Assoc 1933; 25(5): 655-676.
2. Massoudinejad M R, Eslami A, Khashij M. Removal of Mn^{2+} from aqueous solution using Clinoptilolite coated with manganese dioxide. J Saf Promot Inj Prev 2015; 2(4): 265-272. [In Persian]
3. Islam A A, Goodwill J E, Bouchard R, Tobison J E. Characterization of filter media MnOX(S) surfaces and Mn removal capability. J Am water Works Assoc 2010; 102(9): 71-83.
4. Tobiason J E, Bazilio A, Goodwill J, Mai X, Nguyen C. Manganese removal from drinking water sources. Current Pollution Reports 2016; 2(3): 168-177.
5. Zhang Z, Zhang Z, Chen H, Liu J, Liu C, Ni H, et al. Surface Mn(II) oxidation actuated by a multicopper oxidase in a soil bacterium leads to the formation of manganese oxide minerals. Sci Rep 2015; 5:1-13.
6. Chen C, Apul O G, Karanfil T. Removal of bromide from surface waters using silver impregnated activated carbon. Water Res 2017; 113: 223-230.
7. Edwin Vasu A. Surface modification of activated carbon for enhancement of nickel(II) adsorption. J Chem 2008; 5(4): 814-819.
8. Gallios G P, Tolkou A K, Katsoyiannis J A, Stefusova K, Vaclavikoa M, Deliyanni E. Adsorption of arsenate by nano scaled activated carbon modified by iron and manganese oxides. Sustainability 2017; 9(10): 1684-1702.
9. Knocke W, Roman J R, Thompson C P J. Soluble manganese removal on oxide-coated filter media. Am Water Works Assoc 1988; 80(12): 65-70.
10. Morgan J, Stumm W. Colloid-chemical properties of manganese dioxide. J Colloid Sci 1964; 19(4): 347-59.
11. Taffarel S R, Rubio. Removal of Mn^{2+} from aqueous solution by manganese oxide coated zeolite. Miner Eng 2010; 23(14): 1131-1138.
12. Teng Z, Yuan H J, Fujita K, Takaziwa S. Manganese removal by hollow fiber micro-filter. Membrane separation for drinking water. Desalination 2001; 139(1-3): 411-418.
13. Goldstein J, Newbury D, Williams D. X-Ray spectrometry in electron beam instruments. Plenum Press, 1995, New York.
14. Dhoble R M, Lunge S, Bhole A G, Rayalu S. Magnetic binary oxide particles (MBOP): a promising adsorbent for removal of As (III) in water. Water Res 2011; 45(16): 4769-4781.
15. Yakout S M, Sharaf El-Deen G. Characterization of activated carbon prepared by phosphoric acid activation of olive stones. Arabian J Chem 2016; 9: 1155–1162.
16. Dashtinejad M, Samadfam M, Fasihi J, Grayelifumeshkenar F, Sepehria H. Synthesis, characterization, and cesium sorption performance of potassium nickel hexacyanoferrate-loaded granular activated carbon. Part Sci Technol 2014; 32(2): 348–354.
17. Kumar H, Manisha H, Sangwan P. Synthesis and characterization of MnO_2 nanoparticles using co-precipitation technique. Int J Chem Chem Eng 2013; 3(3): 155-160.
18. International center for diffraction data 2017. Available at: www.icdd.com

19. Kordesh K V, Batteries (Manganese Dioxide). Marcel Dekker. 1974, New York.
20. Rodrigues S, Munichndaraiah N, Shukla A K. A cyclic voltammetric study of the kinetics and mechanism of electrodeposition of manganese dioxide and mechanism of electrodeposition of manganese dioxide. J Appl Electrochem 1998; 28(11): 1235- 1241.
21. Nijjer S, Thonstad J, Haarberg GM. Oxidation of manganese(II) and reduction of manganese dioxide in sulphuric acid. Electrochim Acta 2000; 46(2-3): 395-399.
22. Petitiperre J Ph, Comminellis Ch, Plattner E. Oxydation Du $MnSO_4$ en dioxyde de manganese dans H_2SO_4 30%. Electrochim. Acta 1990; 35(1): 281-287.
23. Kao W H, Weiber V J. Electrochemical oxidation of manganese (II) at a platinum electrode. J Appl Electrochem 1992; 22(1): 21-27.
24. Da Silveria A N, Silva R, Rubio. Treatment of acid mine drainage (AMD) in South Brazil. Comparative active processes and water reuse. Int J Miner Process 2009; 93(2): 103-109.
25. Izlen Cifci D I, Meric S. Manganese adsorption by iron impregnated pumice composite. Colloids Surf A Physicochem Eng Asp 2017; 522: 279-286.
26. Alagumuthu G, Veeraputhiran V, Venkataraman R. Adsorption isotherms on fluoride removal: batch techniques. Arch App Sci Res 2010; 2(4): 170-185.